4. S. V. Iordanskii and A. G. Kulikovskii, "On the motion of a fluid containing small particles," Izv. Akad. Nauk, Mekh. Zhidk. Gaza, No. 4 (1977).
5. V. I. Myasnikov, "Statistical model of the mechanical behavior of dispersed systems," in: Mechanics of Multicomponent Media in Technological Processes [in Russian], Nauka, Moscow (1978).
6. A. N. Kraiko and L. E. Sternin, "Theory of the flow of a two-velocity continuous medium with solid or liquid particles," Prikl. Mat. Mekh., 29, No. 3 (1965).
7. Ya. B. Zel'dovich and A. D. Myshkis, Elements of Mathematical Physics [in Russian], Nauka, Moscow (1973).
8. Ya. B. Zel'dovich and A. D. Myshkis, Elements of Applied Mathematics [in Russian], Nauka, Moscow (1972).

CALCULATION OF THE NONEQUILIBRIUM PARAMETERS OF AIR AT THE SURFACES OF MODELS AND IN THE WAKES BEHIND THEM FOR THE CONDITIONS OF AEROBALLISTIC EXPERIMENTS

I. G. Eremeitsev and N. N. Pilyugin

UDC 629.7.018.3

The calculation of the nonequilibrium, quasi-one-dimensional flow of chemically reactive gas mixtures is of practical interest in connection with the study of relaxation processes, obtaining gasdynamic jets for physical measurements, and the investigation of plasma supersonic phenomena in the wake behind a body, etc.

Calculations of chemically nonequilibrium, supersonic, quasi-one-dimensional flows are presented in [1-8] and elsewhere. Here various algorithms are used to solve such problems for flows in nozzles and stream tubes near a body. At present the fields of nonequilibrium parameters at the surfaces of spherically blunted cones are calculated for certain conditions of streamline flow using stream tubes, while calculated results for inviscid flow in wakes are absent. In expansion behind the stern cut of a body, where the gas temperature is sharply reduced, it is necessary to make additional allowance for important reactions with the participation of electrons, negative ions, and polyatomic molecules. Calculations of nonequilibrium parameters in the flow over bodies with surfaces of other shapes, in a wide range of variation of the initial parameters, are also necessary for the comparison and treatment of the results of aeroballistic experiments. However, the absence of calculation methods that are convenient and rapid for execution on computers has prevented making such comparative investigations and giving practical recommendations up to now.

The problem of the flow of a chemically nonequilibrium, partially ionized, multicomponent, inviscid gas from a spherical supersonic source was studied in detail in [9]; from the calculations it is seen that in a number of important cases one can use a constant value of the effective adiabatic index, making it possible to obtain a one-to-one connection between the area of a stream tube and the gas pressure.

In the present paper we give a single algorithm for the computer calculation of the direct and inverse quasi-one-dimensional problems of the flow of chemically nonequilibrium, multicomponent air. The formulation and ways of solving a number of problems of nonequilibrium aerodynamics are discussed on the basis of the calculation method developed.

1. Let us consider the steady quasi-one-dimensional flow of a chemically nonequilibrium gas. The system of dimensionless equations describing such flow has the form [1]

$$\rho v S(x) = 1, \quad \rho v \frac{dv}{dx} = -\frac{dp}{dx}, \tag{1.1}$$

Moscow. Translated from Zhurnal Prikladnoi Mekhaniki i Tekhnicheskoi Fiziki, No. 2, pp. 101-111, March-April, 1986. Original article submitted February 15, 1985.

0021-8944/86/2702-0250$12.50

$$\frac{d}{dx}(h+v^2)=0,\quad \rho v\frac{dc_i}{dx}=W_i,\ i=1,2,\ldots,N, \tag{1.1}$$

$$h=\sum_{i=1}^{N}c_ih_i=\sum_{i=1}^{N}c_i\left(\int_0^T c_{pi}dT+h_i^0\right),\quad c_i=\rho_i/\rho,$$

$$p=\rho Tm_*\sum_{i=1}^{N}\frac{c_i}{m_i},\ \sum_{i=1}^{N}c_i=1,\ [X_i]=\frac{c_i}{m_i}\rho,$$

$$W_i=\frac{l_*}{\rho_*v_*}m_iI_i,\ \sum_{i=1}^{N}a_{ij}X_i\underset{k_{bj}}{\overset{k_{fj}}{\rightleftarrows}}\sum_{i=1}^{N}b_{ij}X_i,\ j=1,2,\ldots,N_r,$$

$$I_i=\sum_{j=1}^{N_r}(b_{ij}-a_{ij})\left\{k_{fj}\prod_{k=1}^{N}[X_k]^{a_{kj}}-k_{bj}\prod_{k=1}^{N}[X_k]^{b_{kj}}\right\}.$$

Here S_*S is the area of a stream tube; l_*x, longitudinal coordinate; v_*v, $\rho_*\rho$, $\rho_*v_*^2p$, $(m_*v_*^2/R_A)/T$, $(v_*^2/2)h$, gas velocity, density, pressure, temperature, and enthalpy; c_i and m_i, mass concentration and molecular weight of the i-th component; N, number of chemical components; R_A, universal gas constant; W_i, rate of formation of the i-th component as a result of chemical reactions and ionization; N_r, number of reactions; k_{fj} and k_{bj}, constants of the forward and back chemical reactions; a_{ij} and b_{ij}, stoichiometric coefficients; $[X_i]$, molar-volumetric concentration of the i-th component; $c_{pi}R_A/2m$, heat capacity of the i-th component at constant pressure; $(v_*^2/2)h_i^0$, specific enthalpy of formation of the i-th component; the characteristic dimensional quantities of the given problem are marked by an asterisk. To close the system (1.1) in the direct problem, the shape of a stream tube, i.e., the dependence of the cross-sectional area S on the longitudinal coordinate x, is assigned, while the variation of the pressure p with respect to x is assigned in the inverse problem.

In Eqs. (1.1) we convert from the longitudinal coordinate x to the coordinate r of expansion of a stream tube by substituting r^2 for S(x).

Then we write the system (1.1) as

$$\rho vr^2=1,\ \rho v\frac{dv}{dr}=-\frac{dp}{dr},\ \frac{d}{dr}(h+v^2)=0, \tag{1.2}$$

$$p=\rho T\sum_{i=1}^{N}\gamma_i,\ \rho v\frac{d\gamma_i}{dr}=\sum_{j=1}^{N_r}\nu_{ij}\Gamma_j\varphi_j,\ i=1,2,\ldots,N,$$

$$\gamma_i=\frac{c_i}{m_i}m_*,$$

$$\Gamma_j=\begin{cases}\dfrac{r_*\rho_*^2}{v_*m_*^2}k_{bj}\rho^2 & \text{for ternary reactions,}\\[2ex] \dfrac{r_*\rho_*}{v_*m_*}k_{bj}\rho & \text{for binary reactions,}\end{cases}$$

where $r_* = f(r)l_*$; $f(r) = dx/dr$. For $f(r) = 1$, the system (1.2) coincides identically with the equations describing nonequilibrium gas flow from a spherical source of radius $r_* = l_*$ [9].

As a result of solving (1.2) with the appropriate initial conditions, all the parameters are obtained in the form of functions of r. To convert to the original x coordinate, we must establish a one-to-one correspondence between x and r. In the direct problem it is established directly from the relation $S(x) = r^2$. In this case f is easily calculated: $f = 2rdx/dS$.

In the inverse problem one assigns the pressure profile p(x), while the function S(x) can be calculated after the entire problem is solved. The solution of the inverse problem can be obtained by solving the equivalent direct problem of flow from a source with a variable radius $r_*(r)$. For this purpose the system (1.2) is solved numerically, while the correspondence between r and x is found from the resulting distribution p(r) from the relation

$$\frac{p(x)}{p_0'}=\frac{p(r)}{p_*}=\gamma_{ef}^*M_*^2p(r). \tag{1.3}$$

In (1.3), γ^*_{ef}, p_*, and M_* are the effective adiabatic index [1], the pressure, and the Mach number at the surface of the source r = 1; p_0' is the pressure at the critical point of the body. From (1.3) we get

$$f(r) = \gamma^*_{ef} M_*^2 \frac{dx}{dp} \frac{dp}{dr},$$

where dp/dx is assigned while dp/dr is found from the solution of (1.2). In the particular case when $\gamma_{ef}(r)$ = const, one can determine dp/dr on the basis of isentropic equations [9]:

$$\frac{dp(r)}{dr} = \frac{2\gamma_{ef} p(r)}{r}\left\{\frac{r^4}{M_*^2}\left[\gamma_{ef} M_*^2 p(r)\right]^{\frac{\gamma_{ef}+1}{\gamma_{ef}}} - 1\right\}^{-1}.$$

In the general case, the derivative dp/dr must be calculated numerically together with the solution of Eqs. (1.2). The pressure distribution at the surface of a blunt axisymmetric body can be obtained either on the basis of the numerical solutions tabulated in [10] or from a modified Newton's equation [11]. The pressure distribution over the surface of a sphere is found with high accuracy from the equation [11]

$$\frac{p}{p_0'} = 1 - 1{,}17\sin^2\theta + 0{,}225\sin^6\theta,\ \theta = \frac{\pi}{2} - \alpha, \tag{1.4}$$

$$p_0' = \left\{1 + \gamma M_\infty^2\left(1 - \frac{\varepsilon}{2}\right)\right\} p_\infty,\ \varepsilon = \rho_\infty/\rho_{s0}.$$

Here γ, M_∞, and ρ_∞ are the ratio of heat capacities, Mach number, and density in the oncoming gas stream; α is the angle between the normal to the body and the horizontal axis. The pressure distribution along the axis of the wake can be found by analogy with a strong cylindrical explosion [11, 12].

If we use this equation from [12] and compare it with Eq. (1.4) for $\theta = \pi/2$ and x' = R, where R is the radius of the sphere, then in the wake behind the sphere we have

$$\frac{p}{p_\infty} = 1 + \frac{\gamma M_\infty^2 k_2(\gamma)\sqrt{\frac{C_x}{2}}}{(x' + x_0')/R},\ \gamma = \gamma_\infty, \tag{1.5}$$

$$\frac{x_0'}{R} = \frac{k_2(\gamma)\sqrt{\frac{C_x}{2}}}{\left(1 - \frac{\varepsilon}{2}\right)0{,}055} - 1,\ \gamma k_2(\gamma) = \frac{\gamma^{\frac{\gamma}{2-\gamma}}}{2^{\frac{4-\gamma}{2-\gamma}}},$$

where C_x is the drag coefficient of the body.

As was shown in [13], smoothing of the pressure in a base region of small size has a weak influence on the solution in the wake. Similar expressions for p(x) can also be obtained for other bodies.

Eliminating the pressure from the momentum and energy equations using the equation of state, and converting to the new independent variable $z = r^{-1}$ and the integration variable v, we finally find

$$\frac{dz}{dv} = \frac{\Phi_2}{\Phi_1},\ \frac{dT}{dv} = \frac{\Phi_3}{\Phi_1},\ \frac{d\gamma_i}{dv} = -\frac{1}{vz^2}\frac{\Phi_2}{\Phi_1}\sum_{j=1}^{N_r} \nu_{ij}\Gamma_j\varphi_j,\ i = 1, 2, \ldots, N, \tag{1.6}$$

$$\Phi_1 = \frac{1}{v}\left[T\left(\sum_{i=1}^{N}\gamma_i\frac{dH_i}{dT}\right)\left\{\frac{2}{z} + \frac{\sum_{i=1}^{N}\frac{d\gamma_i}{dz}}{\sum_{i=1}^{N}\gamma_i}\right\} - \sum_{i=1}^{N}\frac{d\gamma_i}{dz}H_i\right],$$

$$\Phi_2 = 2 - \left(\frac{1}{\sum_{i=1}^{N}\gamma_i} - \frac{T}{v^2}\right)\left(\sum_{i=1}^{N}\gamma_i\frac{dH_i}{dT}\right),\ H_i = \frac{h_i m_i}{m_*},$$

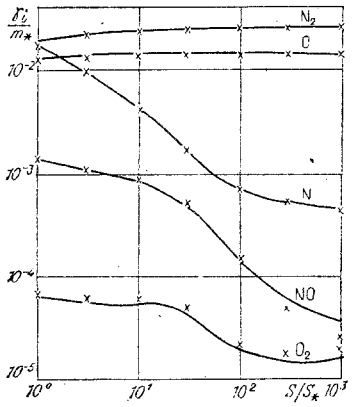

Fig. 1

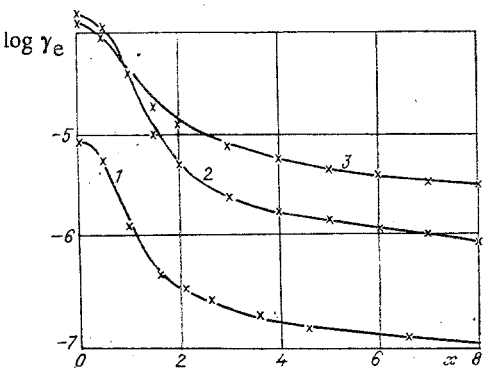

Fig. 2

$$\Phi_3 = \left(\frac{1}{\sum_{i=1}^{N}\gamma_i} - \frac{T}{v^2}\right)\left(\sum_{i=1}^{N}\frac{d\gamma_i}{dz}H_i\right) - 2T\left\{\frac{2}{z} + \frac{\sum_{i=1}^{N}\frac{d\gamma_i}{dz}}{\sum_{i=1}^{N}\gamma_i}\right\}. \tag{1.6}$$

Initial conditions to the system (1.6):

$$v = 1,\ z = 1,\ T = T_* R_A m_*^{-1} v_*^{-2},\ \gamma_i = \gamma_{i*},\ i = 1, 2, \ldots, N.$$

2. The equations are integrated in the restricted region $0 < z \leq 1$ by the transformation of coordinates $z = r^{-1}$. A method of solving the equations analogous to that of [5, 9] was used, making it possible to calculate, by a single implicit-difference scheme with a high accuracy and a sufficiently large step, regions of flow both nearly equilibrium and essentially nonequilibrium.

The system of differential equations (1.6) was replaced by the difference equations

$$\frac{\gamma_{i,m+1} - \gamma_{i,m}}{\Delta v} = -\frac{sW_{i,m+1}}{v_{m+1}z_{m+1}^2}\frac{\Phi_{2,m+1}}{\Phi_{1,m+1}} - \frac{(1-s)W_{i,m}}{v_m z_m^2}\frac{\Phi_{2,m}}{\Phi_{1,m}}, \tag{2.1}$$

$$W_{i,m} = \sum_{j=1}^{N_r}\nu_{ij}\Gamma_{j,m}\varphi_{j,m},\ i = 1, 2, \ldots, N_L,$$

$$\frac{T_{m+1} - T_m}{\Delta v} = s\frac{\Phi_{3,m+1}}{\Phi_{1,m+1}} + (1-s)\frac{\Phi_{3,m}}{\Phi_{1,m}},\ \frac{z_{m+1} - z_m}{\Delta v} = s\frac{\Phi_{2,m+1}}{\Phi_{1,m+1}} + (1-s)\frac{\Phi_{2,m}}{\Phi_{1,m}},$$

where $0 \leq s \leq 1$; Δv is the step of integration; m is the number of nodes of the calculation grid; s is a weight factor; N_L is the number of products of independent reactions. In the calculations we took $s = 0.6$ and $\Delta v = 10^{-3}$. The entire system of nonlinear equations was solved by Newton's method through a standard program.

We analyzed air consisting of 18 components, O, N, e, O_2, N_2, NO, NO^+, O_2^+, N_2^+, O^+, N^+, O_2^-, O^-, NO_2, O_3, N_2O, NO_2^-, O_3^- between which 72 reactions occur. The system of principal chemical reactions was taken in accordance with the recommendations of [1, 3, 8, 9, 14] and is presented in Table 1, where the rate constants of the reactions are given in the form $k = \alpha \cdot 10^n T^b \exp(-C/T)$, the temperature is given in degrees Kelvin, the dimensionality of the reaction rate constants is $(cm^3/mole)^{q-1}\cdot sec^{-1}$ (q is the order of the reaction), and the indices f and b denote the forward and back reactions, respectively. The required equilibrium constants and thermodynamic properties are taken from [14, 15].

3. The calculations of distributions of the nonequilibrium parameters of air by the above method were compared with the results of [2-7], obtained by the method of stream tubes, for both the direct and the inverse problems.

In Fig. 1 we present the distribution of concentrations of the components in the expansion of air in a hypersonic nozzle for $T_* = 10{,}000$ K, $p_* = 5.35\cdot 10^7$ Pa, and $r_* = 1$ cm (lines) from [3]. The shape of the nozzle was assigned in the form

$$S/S_* = 1 + (x/r_*)^2,\ r_* = l_*/\mathrm{tg}\,\theta$$

TABLE 1

j	Reactions	$k_f = a_f 10^{n_f} T^{l_f} e^{-\frac{C_f}{T}}$				$k_b = a_b 10^{n_b} T^{l_b} e^{-\frac{C_b}{T}}$			
		a_f	n_f	l_f	C_f	a_b	n_b	l_b	C_b
1	$O_2 + O_2 \rightleftarrows O + O + O_2$	1,80	21	—1,5	59 500	1,48	18	—1,0	0
2	$O_2 + O \rightleftarrows O + O + O$	4,86	21	—1,5	59 500	4,00	18	—1,0	0
3	$O_2 + N_2 \rightleftarrows O + O + N_2$	4,04	20	—1,5	59 500	3,33	17	—1,0	0
4	$O_2 + N \rightleftarrows O + O + N$	3,64	18	—1,0	59 500	3,00	15	—0,5	0
5	$O_2 + NO \rightleftarrows O + O + NO$	3,64	18	—1,0	59 500	3,00	15	—0,5	0
6	$N_2 + O_2 \rightleftarrows N + N + O_2$	2,00	17	—0,5	113 000	1,10	16	—0,5	0
7	$N_2 + N_2 \rightleftarrows N + N + N_2$	4,92	17	—0,5	113 000	2,70	16	—0,5	0
8	$N_2 + O \rightleftarrows N + N + O$	2,00	17	—0,5	113 000	1,10	16	—0,5	0
9	$N_2 + N \rightleftarrows N + N + N$	2,18	22	—1,5	113 000	1,20	21	—1,5	0
10	$N_2 + NO \rightleftarrows N + N + NO$	2,00	17	—0,5	113 000	1,10	16	—0,5	0
11	$NO + O_2 \rightleftarrows N + O + O_2$	4,06	20	—1,5	75 500	1,00	20	—1,5	0
12	$NO + N_2 \rightleftarrows N + O + N_2$	4,06	20	—1,5	75 500	1,00	20	—1,5	0
13	$NO + O \rightleftarrows N + O + O$	8,12	21	—1,5	75 500	2,00	21	—1,5	0
14	$NO + N \rightleftarrows N + O + N$	8,12	21	—1,5	75 500	2,00	21	—1,5	0
15	$NO + NO \rightleftarrows N + O + NO$	8,12	21	—1,5	75 500	2,00	21	—1,5	0
16	$O + N_2 \rightleftarrows NO + N$	5,92	13	0,0	37 500	1,32	13	0	0
17	$O + NO \rightleftarrows N + O_2$	3,20	9	1,0	19 700	9,56	11	0,5	3 700
18	$N + O \rightleftarrows NO^+ + e$	0,65	12	0,0	31 900	1,80	21	—1,5	0
19	$N_2 + O_2 \rightleftarrows NO + NO$	4,56	24	—2,5	64 600	3,40	21	—2,0	43 100
20	$NO^+ + O_2 \rightleftarrows O_2^+ + NO$	4,40	15	0,0	33 650	5,50	14	0	0
21	$NO^+ + NO \rightleftarrows N_2 + O_2^+$	3,20	8	0,0	11 950	6,00	8	0	0
22	$O + O \rightleftarrows O_2^+ + e$	6,00	8	0,50	80 800	5,00	19	—1,0	0
23	$NO^+ + NO \rightleftarrows O_2 + N_2^+$	1,10	11	0,0	51 530	1,80	10	0	0
24	$NO^+ + N_2 \rightleftarrows NO + N_2^+$	3,80	15	0,0	73 230	2,70	14	0	0
25	$N + N \rightleftarrows N_2^+ + e$	8,50	9	1,0	67 700	5,00	18	—0,5	0
26	$O_2^+ + O \rightleftarrows O^+ + O_2$	3,60	12	0,0	16 480	1,20	13	0	0
27	$NO^+ + O \rightleftarrows O^+ + NO$	1,30	13	0,0	50 130	1,20	13	0	0
28	$NO^+ + N \rightleftarrows N_2 + O^+$	6,40	11	0,0	12 180	1,80	12	0	0
29	$N_2^+ + O \rightleftarrows NO + N^+$	1,80	14	0,0	25 760	6,00	13	0	0
30	$O^+ + N \rightleftarrows N^+ + O$	1,33	15	0,0	10 910	3,00	14	0	0
31	$NO + O_2 \leftarrow NO^+ + O_2^-$					1,20	17	0	0
32	$O_2^- + O_2 \rightleftarrows e + O_2 + O_2$	5,418	9	1,5	4 990	1,445	18	0	0
33	$O_2^- + N_2 \rightleftarrows e + O_2 + N_2$	2,528	8	1,5	4 990	3,02	16	0	0
34	$O_2^- + NO \rightleftarrows e + O_2 + NO$	6,00	7	1,5	5 330	1,00	16	0	0
35	$O^- + O \rightleftarrows e + O_2 + O$	6,00	7	1,5	5 330	1,00	16	0	0
36	$O^- + O \leftarrow e + O + O$					3,02	17	0	0
37	$O^- + O_2 \leftarrow e + O + O_2$					1,445	18	0	0
38	$O^- + NO \leftarrow e + O + NO$					3,02	17	0	0
39	$O^- + N_2 \rightleftarrows e + O + N_2$	2,40	11	1,0	16 900	2,00	18	—0,5	0
40	$O_2 + e \leftarrow O^- + O$					8,428	13	0	0
41	$O_2^- + O \rightleftarrows O_2 + O^-$	4,816	13	0,0	0	2,08	12	0,5	16 200
42	$NO + O \leftarrow NO^+ + O^-$					1,20	17	0	0
43	$NO_2 + N \rightleftarrows NO + NO$	4,00	12	0,0	0	1,08	11	0	39 200
44	$NO_2 + O \rightleftarrows NO + O_2$	1,00	13	0,0	292	1,98	14	—0,5	23 600
45	$NO_2 + e \leftarrow O^- + NO$					1,00	14	0	0
46	$NO_2 + O_2 \rightleftarrows NO + O + O_2$	1,57	17	0,0	36 300	1,45	15	0	—970
47	$NO_2 + N_2 \rightleftarrows NO + O + N_2$	1,57	17	0,0	36 300	1,45	15	0	—970
48	$NO_2 + NO_2 \rightleftarrows NO + NO + O_2$	4,07	12	0,0	13 543	7,25	9	0	0

TABLE 1 (continued)

	Reactions	$k_f = a_f 10^{n_f} T^{l_f} e^{-\frac{C_f}{T}}$				$k_b = a_b 10^{n_b} T^{l_b} e^{-\frac{C_b}{T}}$			
		a_f	n_f	l_f	C_f	a_b	n_b	l_b	C_b
49	$NO_2 + O^- \leftarrow e + O + NO_2$					3,02	17	0	0
50	$O_3 + N_2 \rightleftarrows O + O_2 + N_2$	1,926	15	0,0	12 000	1,27	13	0	—900
51	$O_3 + O_2 \rightleftarrows O + O_2 + O_2$	2,05	15	0,0	12 000	1,486	13	0	—900
52	$O_3 + O_3 \rightleftarrows O + O_2 + O_3$	4,635	15	0,0	12 000	5,436	13	0	—750
53	$NO_2 + O_2 \rightleftarrows O_3 + NO$	6,622	11	0,0	25 100	4,816	11	0	1 200
54	$NO + O_2 \leftarrow O_3 + N$					2,00	10	0	293
55	$O_3 + O \rightleftarrows O_2 + O_2$	8,428	11	0,0	1 500	6,622	12	0	49 600
56	$O_3 + e \leftarrow O_2^- + O$					1,00	14	0	0
57	$N_2O + O \rightleftarrows N_2 + O_2$	6,30	14	0,0	13 437	9,00	11	0,5	53 200
58	$N_2O + O \rightleftarrows NO + NO$	3,63	13	0,0	13 689	2,19	14	0	39 356
59	$N_2O + O \rightleftarrows NO_2 + N$	6,60	15	—1,0	21 100	4,80	12	0	0
60	$NO_2 + N_2 \leftarrow N_2O + NO$					2,512	14	0	25 164
61	$O + NO_2^- \leftarrow O^- + NO_2$					7,20	14	0	0
62	$O_2 + NO_2^- \leftarrow O_2^- + NO_2$					4,316	14	0	0
63	$NO + NO_2 \leftarrow NO^+ + NO_2^-$					1,20	17	0	0
64	$NO_2^- + O_2 \leftarrow O^- + NO + O_2$					1,44	19	0	0
65	$NO_2^- + N_2 \leftarrow O^- + NO + N_2$					7,40	15	0	0
66	$NO_2^- + O \leftarrow O^- + NO + O$					7,40	16	0	0
67	$NO_2^- + NO \leftarrow O^- + NO + NO$					7,40	16	0	0
68	$O_3^- + O_2 \leftarrow e + O_3 + O_2$					1,44	18	0	0
69	$O_3^- + O_2 \leftarrow O_2^- + O + O_2$					5,436	16	0	0
70	$O_2 + O_2 + e \leftarrow O_3^- + O$					8,428	13	0	0
71	$NO_2^- + O_2 \leftarrow O_3^- + NO$					6,00	12	0	0
72	$NO + O_3 \leftarrow NO^+ + O_3^-$					1,20	17	0	0

(a nozzle approximating a conical nozzle with an aperture half-angle θ). The results obtained by the method proposed above are marked by crosses in Figs. 1-4. The good agreement with the data of [3] is seen from Fig. 1. Some disagreement in the NO and O_2 concentrations for $S/S_* > 10^2$ is explained by a difference in the kinetics of the reactions in the present work from what was adopted in [3].

Allowance for a more complete system of reactions leads to a pronounced difference in the distributions of concentrations only for $S/S_* > 10$. Therefore, the simpler system of reactions can be used at small distances from the critical cross section of the nozzle (see [2-7]).

Calculations were made with different pressure distributions in the region behind the cut of the body, where the equations for the pressure at the body and, from the explosion analogy, in the wake are usually "joined," and it was found that a change in the pressure distribution in the near wake has little influence on the results of calculations of the distributions of the nonequilibrium parameters. Thus, a 25% change in the pressure at the distance $x' = x/R \approx 10$ (R is the radius of the middle of the body) behind the body led to a change of less than 1% in the gas temperature and a change of less than 5% in the electron number density per unit volume. This justifies the use of asymptotic equations for the smoothed pressure profile in a region of the near wake of relatively small size.

In Fig. 2 we present distributions of the molar-mass densities γ_e of electrons as functions of the x coordinate (normalized to the radius), taken along the surface of a blunt cone with a blunting radius of curvature R = 15 cm and $\theta = 6°$. Curve 1 corresponds to flow over a body with V_∞ = 4 km/sec at an altitude H = 15 km; 2) V_∞ = 5 km/sec and H = 30 km; 3) V_∞ = 5 km/sec and H = 45 km (results of [7]). A comparison was also made with the data of [2, 4, 6], from which it follows that the proposed method leads to good agreement between the distributions of the nonequilibrium parameters along the axis of a nozzle and over the surface

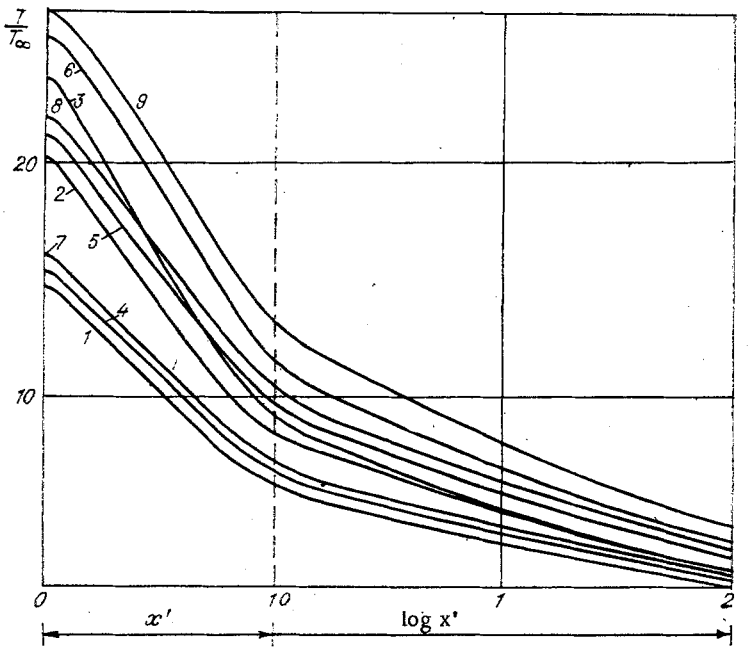

Fig. 3

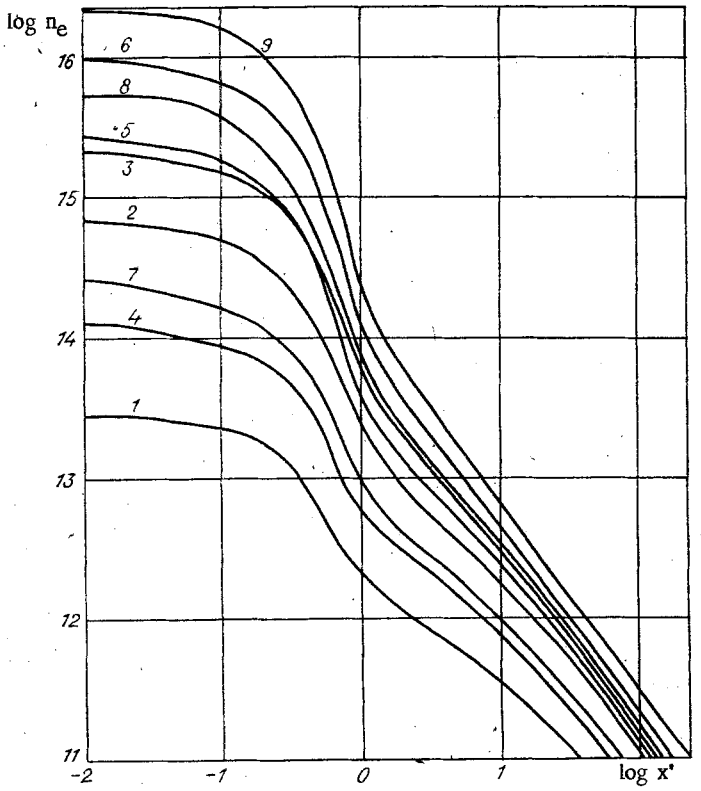

Fig. 4

of a blunt body and the results of numerical calculations of [2-7] for x < 10. For larger distances there is a difference from the data of [2-7] in the distributions of nonequilibrium concentrations. This is connected with the fact that during the expansion of the stream it cools and negative ions and triatomic molecules are formed, so that one must allow for a more complete system of reactions and components than in [2-7].

4. The present calculation method also enables us to determine the distributions of nonequilibrium parameters at the outer boundary of the viscous wake and the initial conditions in the wake behind a model in an aeroballistic experiment.

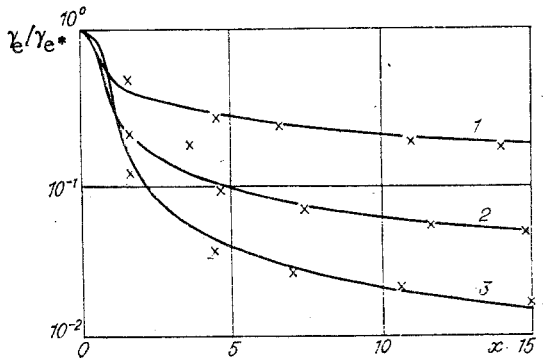

Fig. 5

In Figs. 3 and 4 we present the results of calculations of the nonequilibrium parameters of air at the surfaces of spherically blunted models with a diameter of 0.5 cm and in the near wakes behind them for the characteristic conditions of an aeroballistic experiment (T_∞ = 290 K): 1-9 correspond to V_∞ = 4 km/sec and $p_\infty = 1.33\cdot10^3$ Pa; V_∞ = 5 km/sec and $p_\infty = 1.33\cdot10^3$ Pa; V_∞ = 6 km/sec and $p_\infty = 1.33\cdot10^3$ Pa; V_∞ = 4 km/sec and $p_\infty = 5.33\cdot10^3$ Pa; V_∞ = 5 km/sec and $p_\infty = 5.33\cdot10^3$ Pa; V_∞ = 6 km/sec and $p_\infty = 5.33\cdot10^3$ Pa; V_∞ = 5 km/sec and $p_\infty = 1.07\cdot10^4$ Pa; V_∞ = 5 km/sec and $p_\infty = 1.07\cdot10^4$ Pa; V_∞ = 6 km/sec and $p_\infty = 1.07\cdot10^4$ Pa. The pressure distribution along the axis of symmetry was assigned from Eq. (1.5). The x' coordinate along the axis of symmetry was reckoned from the critical point of the body and was normalized to the blunting radius. The numerical solution in Figs. 3 and 4 is, strictly speaking, valid only up to the point of intersection of the inviscid stream tube with the boundary of the core of the turbulent viscous wake, which comprises several dozen times the diameter of the body. For estimates, however, the results for larger distances are given in Figs. 3 and 4.

Along with the numerical solution presented above, it is important to obtain a simple analytical solution, under certain assumptions, for the electron density distribution in a stream tube.

In [1, 9] it was shown that for nearly equilibrium flow one can introduce an effective constant index γ_{ef}, which enables one to obtain a simple solution. For $1.5 \leq r \leq 15$ we represent it approximately in the form of the functions [16]

$$v(r) = [\eta(r)\, g(M_*)/\varepsilon_1]^{1/2}, \quad \varepsilon_1 = \frac{\gamma_{ef}-1}{\gamma_{ef}+1}, \tag{4.1}$$

$$T(r) = \frac{\gamma_{ef}+1}{2\gamma_{ef}}\,\varepsilon_1^{\frac{\gamma_{ef}-1}{2}}\, r^{2(1-\gamma_{ef})}\, g(M_*),$$

$$\rho(r) = \sqrt{\varepsilon_1/[\eta(r)\, g(M_*)]}\, r^{-2},$$

$$p(r) = \frac{1}{2\gamma_{ef}}\left[(\gamma_{ef}^2-1)\,\varepsilon_1^{\gamma_{ef}-1}\, g(M_*)/\eta(r)\right]^{1/2} r^{-2\gamma_{ef}},$$

$$\eta(r) = 1 - \varepsilon_1^{\frac{\gamma_{ef}-1}{2}}\, r^{-2(\gamma_{ef}-1)}\sigma^{-1}(M_*),$$

$$\sigma(M_*) = \left(\varepsilon_1 M_*^2 + 1 - \varepsilon_1\right)^{\frac{\gamma_{ef}+2}{2}} \Big/ M_*^{\gamma_{ef}-1}, \quad g(M_*) = \left(\varepsilon_1 M_*^2 + 1 - \varepsilon_1\right)/M_*^2.$$

A calculation from Eqs. (4.1) leads to a difference of 1% from the exact numerical results for the velocity profiles and of 8% for the temperature in the range of $1.5 \leq r \leq 15$. For simplicity, we assume that electron recombination in the reaction $e + NO^+ \to N + O$ occurs from the critical point of the body along a stream tube. Then we write the equation for the molar-mass density γ_e as

$$\rho v \frac{d\gamma_e}{dx} = -\frac{K_0}{m_*}\frac{\gamma_e^2\rho^2}{T^{3/2}}, \quad \gamma_e(x=0) = \gamma_{e*}, \tag{4.2}$$

where m_* is the molecular weight; $K_0 = 1.8\cdot10^{21}$ cm$^3\cdot$K$^{3/2}$/(mole·sec); $n_{e*} = \gamma_{e*}p_*/kT_*$; parameters at the stagnation point are marked by an asterisk.

We introduce the dimensionless parameters

$$\bar{v} = v/v_*, \ \bar{\rho} = \rho/\rho_*, \ \bar{x} = x/R, \ \bar{T} = T/T_*. \tag{4.3}$$

In Eq. (4.2) we change to the r coordinate (we omit the asterisk):

$$v\frac{d\gamma_e}{dr} = -\frac{K_0}{m_*}\frac{\gamma_e^2\rho(r)f(r)}{[T(r)]^{3/2}}, \ f = \frac{dx}{dr}, \ \gamma_e(r=1) = \gamma_{e*}. \tag{4.4}$$

The solution of Eq. (4.4) is reduced to the form

$$\frac{\gamma_e(r)}{\gamma_{e*}} = \left\{1 + \frac{K_0}{m_*}\frac{\gamma_{e*}\rho_* R}{v_* T_*^{3/2}}F(r)\right\}^{-1}, \ F(r) = \int_1^r \frac{\rho(r)f(r)\,dr}{v(r)[T(r)]^{3/2}}. \tag{4.5}$$

The correspondence between x and r is established through the relation [9]

$$r^2 = \left\{[p(x)]^{1/\gamma_{ef}}\sqrt{1 + \lambda_* - \lambda_*[p(x)]^{\frac{\gamma_{ef}-1}{\gamma_{ef}}}}\right\}^{-1}, \ \lambda_* = \frac{2}{(\gamma_{ef}-1)M_*^2}.$$

Using (4.1), for r ≥ 2.5 (x ≥ 1.6) we obtain

$$F(r) = A(\gamma_{ef}) + B(\gamma_{ef})I(r), \ I(r) = \frac{t}{y}\left(1 + \frac{2t^2}{3y^2} + \frac{t^4}{5y^4}\right), \tag{4.6}$$

$$y = r^{1-\gamma_{ef}}, \ t = \sqrt{a^2 - y^2},$$
$$a^2 = \varepsilon_1^{\frac{1-\gamma_{ef}}{2}}\sigma(M_*).$$

For flow over a spherically blunted model, a comparison with exact calculations for $\gamma_{ef} \approx 1.2$ gave A = −0.806 and B = 0.642.

The results of exact calculations of $\gamma_e(x)$ can differ severalfold from calculations based on Eqs. (4.5) and (4.6) for x' ≈ 1. This difference is connected with the use of only one recombination reaction in the analytic solution (4.5), whereas a larger number of reactions with charged particles actually influence the electron density. Therefore, within the framework of one principal model recombination reaction, we introduce the effective value K_{0ef} of the reaction rate constant, which allows for the influence of the remaining (neglected) reactions. A comparison with exact calculations for $10 \leq M_\infty \leq 20$ and $1.33\cdot10^3$ Pa ≤ p_∞ ≤ $1.33\cdot10^4$ Pa gives

$$K_{0ef} = (-0.86M_\infty + 26.58)(-0.005p_\infty + 1.17)\cdot10^{20}\ \text{cm}^3\,K^{3/2}/(\text{mole}\cdot\text{sec}).$$

The dependence $\gamma_e(x)/\gamma_{e*}$ for a sphere of R = 0.25 cm is constructed in Fig. 5, where 1 is the numerical results for M_∞ = 11.7 and $p_\infty = 1.07\cdot10^4$ Pa; 2) M_∞ = 14.7 and $p_\infty = 5.33\cdot10^3$ Pa; 3) M_∞ = 17.6 and $p_\infty = 1.07\cdot10^4$ Pa. The results of calculations from Eqs. (4.5) and (4.6) are plotted there for comparison; the good agreement is seen.

5. Let us consider the formulation of new variational problems of nonequilibrium aerodynamics in more detail. In the motion of models at hypersonic velocities, highly excited quantum states of atoms and molecules, as well as charged particles, are formed in the shock layer and the wake behind the body. The presence of charged particles (mainly electrons) and radiating components enables one to carry out shf diagnostics and optical measurements in the gas stream near a flying model in an aeroballistic experiment. The integral intensity of optical or shf signals in a recording is determined by the flow regime and the geometrical dimensions and shape of the body. In this connection we pose a problem: to find the shape of the body from the condition that a certain functional J, dependent on some concentration, be minimal for different isoperimetric conditions.

Let the origin of coordinates be located at the critical point of the axisymmetric body, the OX axis be directed along its axis of symmetry, and the OY axis be perpendicular to the OX axis. The equation describing the shape of the body in these coordinates is y = y(x), with y(0) = 0.

The following functionals J, dependent on the shape y = y(x) of the axisymmetric body, can be chosen in different problems:

$$J = c_i(x = L), \tag{5.1}$$

where c_i is the mass concentration of the i-th component, determining the process under consideration; L is the length of the body [the functional (5.1) depends on the shape of the body in a complex way through the pressure distribution over its surface];

$$J = 2\pi \int_0^{\Delta_s(L)} \rho u c_i y dz_s \tag{5.2}$$

where J expresses the flux of the i-th component through the shock layer of thickness Δ_s; ρ and u are the gas density and velocity; z is the coordinate along the normal to the surface of the body [Eq. (5.2) determines the solution of the equations describing the flow in a viscous turbulent wake];

$$J = S_1^{-1} \int_{S_1} c_i ds. \tag{5.3}$$

Here ds is an element of the lateral surface of the body; S_1 is the area of the frontal part of the body; J expresses the average value of the i-th concentration over the surface of the body. The solutions of variational problems on the body with the minimum value of one of the functionals (5.1)-(5.3) are obtained for different combinations of the length, the radii of the nose and middle, the volume, and the lateral surface area of the body on the basis of the method developed above, jointly with the method of local variations.

Determining the optimum shapes of bodies in the indicated sense enables one to reduce (or increase) the radiation intensity and the amount of charged particles near models and in the wakes behind them, which is important in recording the physical processes in aerobalistic experiments.

LITERATURE CITED

1. V. P. Agafonov, V. K. Vertushkin, A. A. Gladkov, and O. Yu. Polyanskii, Nonequilibrium Physicochemical Processes in Aerodynamics [in Russian], Mashinostroenie, Moscow (1972).
2. J. J. Martin, Atmospheric Reentry: An Introduction to Its Science and Engineering, Prentice-Hall, Englewood Cliffs, New Jersey (1966).
3. J. A. Lordi and R. E. Mates, "Nonequilibrium effects of high-enthalpy expansions of air," AIAA J., 3, No. 10 (1965).
4. L. I. Skurin, "On the modeling of an air plasma on a ballistic path in a mixture of air with a heavy gas," Zh. Tekh. Fiz., 50, No. 4 (1980).
5. V. N. Kamzolov and U. G. Pirumov, "Calculation of nonequilibrium flows in nozzles," Izv. Akad. Nauk SSSR, Mekh. Zhidk. Gaza, No. 6 (1966).
6. V. P. Stulov and V. P. Shkadova, "One-dimensional nonequilibrium air flows," Izv. Akad. Nauk SSSR, Mekh. Zhidk. Gaza, No. 2 (1968).
7. G. N. Sayapin, "Nonequilibrium electron densities at the surfaces of thin blunt cones in a supersonic air stream," Tr. Tsentr. Aerogidrodin. Inst., No. 1656 (1975).
8. I. H. Spurk, M. Gerber, and R. Sedney, "Characteristic calculation of flowfields with chemical reactions," AIAA J., 4, No. 1 (1966).
9. I. G. Eremeitsev, N. N. Pilyugin, and S. G. Tikhomirov, "Nonequilibrium air flow from a supersonic spherical source," in: Hypersonic Flows in Flow over Bodies and in Wakes [in Russian], G. G. Chernyi and G. A. Tirskii (eds.), Moscow State Univ. (1983).
10. Yu. N. D'yakonov, L. V. Pchelkina, and I. D. Sandomirskaya, Supersonic Flow over Blunt Bodies [in Russian], Moscow State Univ. (1971).
11. V. V. Lunev, Hypersonic Aerodynamics [in Russian], Mashinostroenie, Moscow (1975).
12. L. I. Sedov, Similarity and Dimensional Methods in Mechanics, Academic Press, New York (1959).
13. S. C. Lin and T. E. Hayes, "A quasi-one-dimensional treatment of chemical reactions in turbulent wakes of hypersonic objects," AIAA J., 2, No. 7 (1964).
14. Sang-Wook Kang, "Nonequilibrium, ionized, hypersonic flow over a blunt body at low Reynolds number," AIAA J., 8, No. 7 (1970).

15. V. P. Glushko, L. V. Gurvich, et al., Thermodynamic Properties of Individual Substances [in Russian], Nauka, Moscow (1978).
16. I. G. Eremeitsev and N. N. Pilyugin, "Friction and heat exchange in laminar and turbulent boundary layers in nonequilibrium supersonic flow over axisymmetric bodies," Izv. Akad. Nauk SSSR, Mekh. Zhidk. Gaza, No. 2 (1984).

INTENSELY RADIATING, SUPERCRITICAL SHOCK WAVES

I. V. Nemchinov, I. A. Trubetskaya, and V. V. Shuvalov

UDC 533.6.011.72

The quasisteady structure of strong, intensely radiating shock waves propagating at a velocity D in a gas with a density ρ_0 and the laws of variation of their brightness temperatures T_ε with variation of D were investigated in [1, 2]. The role of emission is characterized by the parameter $\eta = q_b/q_h$, where q_b is the emission flux of a black body at the temperature T_s corresponding to the velocity D in accordance with the shock adiabat, q_h is the hydrodynamic flux of energy through the shock wave front, with $q_b = \sigma T_s^4$, while $q_h = (1/2)\cdot \rho_0 D u_s^2$ (σ is the Stefan–Boltzmann constant and u_s is the gas velocity behind the shock wave front). Subcritical (in the terminology of [1, 2]) shock waves, i.e., those for which $\eta < 1$, are usually used as emission sources [3].

Only the soft part of the radiation emitted by the gas behind the front travels to large distances from the front. The hard part of this radiation is absorbed immediately ahead of the front, forming a heated layer. In [1-3], the value I_1 of the first ionization potential of the working gas is taken as the arbitrary boundary ε_1 separating the spectrum into these parts. We note that, according to calculations [4, 5] and measurements [6, 7] of the total emission flux, ε_1 is 1-2 eV lower than I_1 owing to absorption in broadened lines in the heated layer. As the velocity D of the front and the parameter η increase, the maximum temperature T_- ahead of the wave front grows. Absorption also begins in the long-wavelength part of the spectrum. Only quanta emitted in the heated layer itself emerge. The brightness temperatures T_ε and the thermal-radiation fluxes q_r at first follow T_s and q_b and then, having reached maxima, decrease [1-7].

In subcritical shock waves the highest values of q_r and T_ε can be obtained by using helium and neon, which have the highest values of I_1, as the working gases. In neon, for example, according to calculations [4, 5] and measurements [6-8], they reach 9-10 eV and 200-400 MW/cm^2 at velocities of 50-70 km/sec. Higher temperatures T_s can be attained when heavier gases are used. The equation of state for xenon [9], for example, can be approximated by the power function

$$e = AT^{a}\delta^{-\alpha}, \quad \delta = \rho/\rho_L, \tag{1}$$

where e is the internal energy per unit mass, kJ/g; ρ and ρ_L are the density and standard density of xenon (5.89 mg/cm^3); A = 4.0; a = 1.65; α = 0.14 in the temperature range T = 2-30 eV. Hence,

$$T_s = 0{,}35u_s^{1{,}21}\delta_0^{0{,}085}, \ \eta = 0{,}47\cdot 10^{-2}u_s^{1{,}81}\delta_0^{-0{,}66}. \tag{2}$$

Here u_s is in km/sec; T_s is in eV; $\delta_0 = \rho_0/\rho_L$. At a velocity u_s = 40 km/sec, according to (2), we obtain T_s = 30 eV for δ_0 = 1 and the back-body emission flux q_b is 88 GW/cm^2. In reality, however, shock waves are supercritical starting with u_s = 19 km/sec and T_s = 13 eV, while the maximum fluxes q_r^m are already reached for subcritical waves and, according to [6, 7] comprise 15-20 MW/cm^2, corresponding to an effective temperature $T_e = (q_r^m/\sigma)^{1/4}$ = 3.0-3.5 eV. Thus, screening of the front prevents attaining high velocities and effective temperatures and obtaining large fluxes of radiation escaping from the front "to infinity."

Moscow. Translated from Zhurnal Prikladnoi Mekhaniki i Tekhnicheskoi Fiziki, No. 2, pp. 112-119, March-April, 1986. Original article submitted February 14, 1985.

0021-8944/86/2702-0260$12.50